NASA TECHNICAL NOTE

NASA TN D-4101

NASA TN D-4101

ACTIVATION, GROWTH, AND DETACHMENT OF BOILING BUBBLES IN WATER FROM ARTIFICIAL NUCLEATION SITES OF KNOWN GEOMETRY AND SIZE

by John R. Howell and Robert Siegel

Lewis Research Center

Cleveland, Ohio

NATIONAL AERONAUTICS AND SPACE ADMINISTRATION • WASHINGTON, D. C. • AUGUST 1967

NASA TN D-4101

ACTIVATION, GROWTH, AND DETACHMENT OF BOILING BUBBLES IN WATER FROM ARTIFICIAL NUCLEATION SITES OF KNOWN GEOMETRY AND SIZE

By John R. Howell and Robert Siegel

Lewis Research Center
Cleveland, Ohio

NATIONAL AERONAUTICS AND SPACE ADMINISTRATION

For sale by the Clearinghouse for Federal Scientific and Technical Information
Springfield, Virginia 22151 – CFSTI price $3.00

ACTIVATION, GROWTH, AND DETACHMENT OF BOILING BUBBLES IN WATER FROM ARTIFICIAL NUCLEATION SITES OF KNOWN GEOMETRY AND SIZE

by John R. Howell and Robert Siegel

Lewis Research Center

SUMMARY

Artificial nucleation sites in the range from 0.0015 to 0.032 inch in radius were drilled in a polished metal surface by either electron-beam or mechanical drilling. The formation of boiling bubbles was studied by electrically heating the surface in saturated distilled water and by obtaining surface temperature, heat flux, and photographic data. The surface-temperature elevation above saturation required to produce ebullition from a pre-existing vapor nucleus is given as a function of site radius. The results are compared with several available analyses including one proposed in the present report. The analyses do not compare well with the data, thus a basic feature is still missing from the analytical models. In general, the analyses predict that bubbles will start to grow at surface temperatures lower than those measured experimentally. Data giving bubble growth as a function of site radius and surface temperature elevation are provided for saturated water and are compared with theoretical growth relations. At bubble detachment in saturated liquid, the buoyancy and surface-tension forces are found to be approximately equal.

INTRODUCTION

The boiling phenomena have been the subject of numerous research efforts as surveyed, for example, in references 1 and 2. These investigations have revealed that many factors affect boiling, and, at present, there is no correlation for heat-transfer coefficient that satisfactorily accounts for all parameters involved. As a consequence, some recent research has been undertaken with the view that a quantitative understanding of the boiling problem will be achieved only by a return to very basic studies of the boiling process, starting with the formation of individual bubbles and their growth and departure. The conditions under which bubbles will be produced from a specified cavity are the principal subject of the present report.

Analytical predictions of the criteria for the initiation of bubble growth have been made in references 3 to 7, but only limited experimental data are available (refs. 5 and 8 to 11) that relate bubble formation to a known site size and geometry. A satisfactory verification of these analyses has therefore not been possible. The analyses of bubble incipience criteria by Hsu (ref. 3) and by Han and Griffith (ref. 4) are quite similar. Both are based on the assumption that a surface cavity has a hemispherical vapor cap over it that serves as a bubble nucleus, and both assume that this nucleus will begin to grow only when the thermal layer of superheated liquid adjacent to the surface is of a sufficient thickness. The chief difference in the two analyses is in the assumption of how large the thermal-layer thickness must be to produce growth for a vapor nucleus of a given height. With an assumed relation between the thermal-layer thickness and the bubble nucleus size at incipience, a relation between active cavity size and surface-temperature elevation is derived. The transient conduction equation is used to provide the temperature distribution in the thermal layer, and the required temperature difference for bubble growth is found from the Clausius-Clapeyron equation. In reference 3, the range of active cavity size is given for a known surface-temperature elevation above saturation or for a specified constant heat flux at the wall. Reference 4 discusses the case of specified surface temperature.

Griffith and Wallis (ref. 5), among others, used the Clausius-Clapeyron equation and the Gaussian expression relating surface tension and radii of curvature to the pressure difference across the bubble interface to determine the active cavity radius. In contrast with the results of references 3 and 4, this relation does not indicate a maximum cavity size and predicts that only small values of the temperature difference between the wall and the saturated liquid are required to initiate bubble growth as the cavity radius becomes large. The derivation is based on having a liquid of uniform temperature surrounding the bubble, and the liquid must be superheated for the bubble to grow. The relations given in references 3 and 4 do not have the restriction of a uniform liquid temperature.

For a heated surface in a saturated bulk liquid, Madejski (ref. 6) includes the effect of the temperature gradient around the bubble causing a variation of bubble curvature. The wall- to saturated-liquid-temperature difference at incipience is found to be that predicted in reference 5 multiplied by a factor larger than one. For the conditions of the present experiments, the factor produced negligible change from the results of reference 5.

Leont'ev and Kirdyashkin (ref. 7) provide an analysis based on free-convection theory for predicting the thickness of a thermal layer on a horizontal surface. The thickness is predicted to depend on the temperature difference between surface and bulk fluid to the minus one-third power. This thermal-layer thickness is then inserted into

the incipience analysis of Hsu (ref. 3) to predict the dependence of active cavity radius upon temperature.

The actual trend with cavity radius of wall- to saturated-liquid-temperature difference at incipience has not been completely resolved experimentally. As shown in references 5 and 11, the predicted incipience temperature differences are generally lower than those observed experimentally. In the work reported in reference 5, cavities 0.0027 inch in diameter were pricked in a surface with a sharpened needle. The cavities produced bubbles at a surface superheat of 20° F compared with a value of 3° F as predicted by the analysis of reference 5. In reference 11, cavities with diameters from 0.001 to 0.005 inch were formed by etching with acid. For water at atmospheric pressure, the measured surface superheats required to provide bubbles were about 14° F compared with their predicted values of 2° to 4° F.

Since the activation theories postulate that a vapor nucleus is initially present, they apply only to a range of cavity sizes in which vapor (or gas) is entrapped. The maximum cavity diameter thus should be limited to the value which will not allow replacement of vapor within the cavity by the surrounding liquid. Bankoff (ref. 12) presents a method by which this size may be established for certain systems.

The present study was undertaken to determine experimentally the surface-temperature elevation above saturation required for a cavity to become active. Because of the many parameters which could affect the system, a simple configuration was chosen for the heated surface and cavity. Yatabe and Westwater (ref. 10) have indicated that cavity shape appears to have little effect on nucleating characteristics; thus, the only cavity parameter varied systematically in the present study was the diameter. The only system parameter varied was surface temperature (and therefore, of course, surface heat flux). The water was at saturation for all the tests. In addition to cavity activation data, high-speed motion pictures were taken at and near incipience of bubble formation to study the nature of the vapor nucleus and the bubble growth and departure characteristics from sites of known size and geometry.

An earlier version of this report is given by reference 13.

APPARATUS

Heated Test Sections

The test specimens were made from number 410 stainless-steel strips, 4 inches long, 1/2 inch wide, and 1/16 inch thick. This alloy was chosen for its magnetic properties which allowed fine polishing on available equipment that utilized magnetic clamps. The strips were polished on all edges and on one face to achieve a finish with

root mean square roughness less than 4 microinches. After polishing, a 20-gage Chromel-Alumel thermocouple was spotwelded to the center of the unfinished face of the specimen. The thermocouple leads were run parallel to the strip to reduce conduction losses. The strip was then placed in a mold which left only the finished face exposed, and epoxy resin was cast around the remaining sides providing a block of thermal insulation 4 by 1 by 1/2 inches. The artificial nucleation sites were drilled into the polished face, and the entire specimen was cleaned ultrasonically in an alcohol bath and finally in a distilled-water bath.

Artificial Sites

Two types of artificial sites were studied. The first type was drilled by an electron-beam disintegration technique in the hope of producing extremely small diameters. However, the smallest site diameter attained by this method was 0.0025 inch. In addition, the disintegration technique tended to leave a cratered area outside the actual hole diameter. This technique left some doubt as to the exact geometry of the cavity. The cavity depths ranged from 0.003 to 0.019 inch. A photograph of a typical cavity is shown in figure 1(a).

The second type of artificial site was produced by a mechanical drill for the smaller holes and by an end mill for the larger diameters. These methods produced holes that were quite round at the surface and with no cratering evident (figs. 1(b) and (c)). Diameters near a minimum of 0.003 inch were attained by this method using drills of 0.002-inch nominal diameter. The largest diameter tested was 0.064 inch. The cavity depths were from 0.010 to 0.020 inch.

In most of the test strips, two sites of the same nominal diameter were drilled about 1 inch apart. Three strips were tested where either four or six holes of various diameters were drilled about 3/4 inch apart in a staggered pattern into the same strip; thus, the effect of site diameter could be observed while all the sites were under identical conditions.

The diameters of the cavities were measured using a metallograph, an optical device with a calibrated eyepiece, and the accuracy was estimated as ±0.0002 inch for mechanically drilled sites. The photographs in figure 1, obtained using the metallograph, give a representation of the view seen through the calibrated eyepiece. Accuracy of the measurements for the electron-beam sites was about ±0.0005 inch; the error was greater than for the mechanically drilled sites because of the uncertainty introduced by the cratering.

Cavity depths were measured during the drilling process. A depth gage on the precision drill press provided this measurement for the mechanically drilled cavities

while the expended energy and time of disintegration were used to estimate the depths of the holes obtained by electron-beam disintegration.

Pool Boiler

The boiler consisted of a cylindrical stainless-steel tank, 14 inches in diameter and 30 inches high (fig. 2). Two 8-inch-diameter quartz windows were provided diametrically opposite each other for viewing or photography. Four 1000-watt heaters near the bottom of the tank provided auxiliary heat to maintain saturation conditions within the boiler. Two Chromel-Alumel thermocouples were immersed in the boiling fluid to monitor the bulk temperature. Power was provided through copper electrodes extending down through the boiling water. The test specimen was clamped to the electrodes with the test surface horizontal. The outer surface of the boiler, including the bottom, was wrapped with 2 inches of felt insulation.

Auxiliary Equipment

Power was supplied from a motor-controlled variable output alternating-current transformer. The alternating current provided to the test specimen produced no problems in the temperature measuring system. Calculations based on the analysis of reference 14 showed that the strip geometry and physical properties were such that temperature fluctuations resulting from the 60-cycle current were negligible.

A high-speed camera with the associated timing equipment and lighting was available for photographing individual sites. Lenses and extension tubes were so arranged that the individual bubbles were magnified to practically fill the frame of the film.

Instrumentation

The current and the voltage across the test section were read with 1/4 percent alternating-current meters. The bulk water and test specimen thermocouple voltages were read on a laboratory-type potentiometer. The thermocouples were referenced to a $150^{\circ} \pm 1/4^{\circ}$ F commercial thermocouple reference oven.

PROCEDURE

The boiler tank was drained and cleaned after every second day of experimentation.

An ultrasonically cleaned test specimen was clamped to the electrodes, and the tank was raised into position around the specimen. The boiler was then filled with distilled water, and the auxiliary heaters were turned on. The water was heated to saturation and was allowed to boil for a few hours to drive off any absorbed gases. The power to the auxiliary heaters was decreased to a level sufficient to maintain saturation while reducing the convective eddies formed by the boiling from these heaters.

Power at a low level was then applied to the specimen, and the bulk temperature, current and voltage across the specimen, and specimen thermocouple readings were taken. Note was made as to whether the artificial site or sites were active, and the level of activity was observed (none, sporadic, intermittent, steady, etc.). The power was then increased several percent, and new readings were obtained. This process was continued until the artificial sites were producing bubbles continuously (except for a few cases where no nucleation occurred from sites that were previously active, possibly because the sites became filled with water). The power level was then reduced in steps of several percent each until all activity ceased.

Photographs were taken when desired as the tests were too numerous to photograph every test condition.

The surface temperature of the specimen was determined when the activity of the site was steady, was intermittent, or ceased, while the power was either increased or decreased. Thermocouple readings, which were taken on the back (insulated) side of the strip, were used to determine the temperature at the surface by assuming a one-dimensional heat-conduction process through the specimen thickness. For a plate of thickness a, insulated on one side and having uniform internal heat generation, the temperature difference between the two sides is given by

$$T_w - T_o = \frac{qa}{2k} \tag{1}$$

where T_o for the present experiments corresponds to the value provided by the specimen thermocouple. (All symbols are defined in appendix A.)

RESULTS

Activation of Nucleation Sites and Incipience of Boiling

Definition of incipience point. - As shown by Hsu in the discussion appended to reference 13, a distinction must be made between the conditions necessary to cause a bubble nucleus to grow and the more stringent conditions necessary not only for growth

of the nucleus but also for detachment of the bubble from the site. The former will be termed "site activation" and the latter "incipience of boiling."

For a saturated system, the difference between the activation and incipience conditions will be small, because once a nucleus begins to grow it tends to continue its growth (if the thermal layer thickness does not decrease) until detachment occurs. For a subcooled condition, however, incipience may require a significantly higher surface temperature elevation above T_{sat} than that required for bubble activation. Activation thus occurs at the lower limit of conditions necessary for incipience.

The word incipience has been defined in a number of other ways when applied to boiling. One common definition is that incipience corresponds to the surface- to bulk-temperature difference at which the curve of ΔT plotted against the heat flux for the entire surface begins to deviate from the free convection curve. Such a definition has little value in studying bubble production from individual sites involving isolated locations on the surface.

Incipience can also be defined as the condition when the waiting time between departure and initiation of a new bubble is not infinitely long. For the present experiments, however, this definition also has little meaning as each departing bubble left a vapor nucleus behind, and hence the waiting time was always zero.

Hsu (ref. 3) and Han and Griffith (ref. 4) in their analyses consider site activation; that is, the conditions and temperature difference at which a given bubble nucleus begins to grow. This criterion is more valid for the lower limit of incipience in the experiments reported herein, but it still has some inherent difficulties. As the test-section surface temperature was increased, a point was reached where a bubble would grow at the nucleation site and then remain attached to the surface. This condition is one where the vapor nucleus grew and hence was active, but it still did not appear to be incipient boiling as a succession of bubbles was not produced from the site. At a slightly higher temperature level, the bubble detached, and a new bubble began to grow; but this bubble might linger at the surface for many seconds before detaching. For a larger test-surface temperature, the production of bubbles became more regular. Finally, at a still larger temperature difference, bubble production was so regular that a steady stream of bubbles appeared from the cavity. This leads to the following question: Which of these bubble-formation conditions and its corresponding surface- to saturation-temperature difference corresponds to incipience?

Because the irregularities in the nucleation phenomena may be due to the statistical fluctuations inherent in the thermal boundary-layer thickness, it could be conjectured that steady or regular bubble production could only occur when the superheated thermal-layer thickness reached a mean value which was greater than that used in the activation criteria of references 3 and 4.

In the present study, the incipience point was examined with regard to two definitions

One definition that provided an upper limit was that incipience corresponds to the value of ΔT at which regular bubble production occurred from a given site. It is obvious that such a definition involves possible errors in the judgement of the observer and may produce $(\Delta T)_i$ values above the theoretical site activation predictions. It also involves the experimental difficulty of defining when "regular" production is occurring from sites of differing size. If a large and a small site are compared in the region of incipience, the frequency of bubble emission is lower for the larger site as this site is producing larger bubbles; however, the percentage variations around a given mean bubble frequency seemed smaller for large sites. Thus, a small site producing bubbles might not be incipient according to this definition because of a lack of bubble regularity, while a large site producing bubbles at a lower frequency with bubble regularity would meet this incipience criterion.

The second definition of incipience examined experimentally was that it corresponds to the minimum ΔT at which bubbles still grow and detach from the surface. Below this ΔT a bubble might still be present at a site, but it would remain attached to the surface. This criterion would be expected to correspond more closely with a theory predicting site activation but with no consideration as to whether a stream of bubbles is produced. For this definition of incipience, the thermal boundary-layer thickness will just occasionally, on a statistical basis, reach the required thickness for bubble growth and detachment.

Incipience of nucleation in saturated water. - The data, listed in table I, for the surface- to bulk-temperature difference $(\Delta T)_i$ at which steady emission occurred according to the first definition of incipience are plotted as a function of site radius R_c in figure 3(a). The $(\Delta T)_i$ from the second definition are given in figure 3(b). The points presented in figure 3(a) are those $(\Delta T)_i$ values at which emission appeared to be steady but for which the next step decrease of about 10 percent in heat flux caused extinction or an extreme decrease of the rate of bubble production from the site. In figure 3(b), the $(\Delta T)_i$ were taken when just a very few bubbles were being produced. Where a range is shown about a data point, the lower limit produced no detaching bubbles while the upper limit provided a few bursts of bubbles on the order of 10 to 20 seconds apart. The incipience temperatures obtained when increasing heat flux generally were higher in value for a given site radius and had more scatter. The values obtained during increasing heat flux are not shown. The fluid bulk was maintained at a saturated boiling condition for all the data in figure 3.

For a specific individual site, a range in the emission behavior would be expected as is characteristic of boiling processes. As shown in figure 3, the range was of the order of several degrees. At each site radius, the minimum $(\Delta T)_i$ may be regarded as corresponding to conditions most favorable to bubble growth. When making comparisons with theory, the envelope through the minimum $(\Delta T)_i$ points should be kept in mind

since it delineates the boundary between the inactive region and the region of possible activity.

Comparison of saturated data with analyses of incipience. - The analyses of Han and Griffith (ref. 4), Hsu (ref. 3), and Griffith and Wallis (ref. 5) predict respectively the following relations for the range of active cavity radius R_c as a function of temperature of the heated surface T_w. From reference 4,

$$(R_c)_{max,\,min} = \frac{\delta}{3}\frac{(T_w - T_{sat})_i}{(T_w - T_{bulk})_i}\left\{1 \pm \left[1 - \frac{12(T_w - T_{bulk})_i}{(T_w - T_{sat})_i^2}\frac{T_{sat}\sigma}{\delta\rho_v\lambda}\right]^{1/2}\right\} \tag{2}$$

From reference 3,

$$(R_c)_{max,\,min} = \frac{\delta}{2C_1}\frac{(T_w - T_{sat})_i}{(T_w - T_{bulk})_i}\left\{1 \pm \left[1 - \frac{8(T_w - T_{bulk})_i}{(T_w - T_{sat})_i^2}C_3\frac{T_{sat}\sigma}{\delta\rho_v\lambda}\right]^{1/2}\right\} \tag{3}$$

where the constants C_1 and C_3 are functions of the bubble-surface contact angle and the angle between the surface and the tangent to the cavity mouth. From reference 5,

$$R_c = \frac{2\sigma T_{sat}}{\lambda\rho_v(T_w - T_{sat})_i} \tag{4}$$

The most simple of these as given in equation (4) and a modified form as given in reference 6 have the possible shortcoming of predicting no maximum active cavity size. A plot of equation (4) in figures 3(a) and (b) shows that it does lie to the left of all the data, but the $(\Delta T)_i$ values are smaller than those observed. At large site radii, the deviation becomes larger since the data tend toward larger $(\Delta T)_i$ while equation (4) predicts a decrease of $(\Delta T)_i$ with increasing site radius.

The analyses of Hsu (ref. 3) and of Han and Griffith (ref. 4) require a knowledge of the thermal-layer thickness. For saturated water, this thickness has been experimentally measured by Marcus and Dropkin (ref. 15) who provide a correlation between thermal-layer thickness and heat-transfer coefficient. For values of heat-transfer coefficient in the range of the present experiments (350 to 650 Btu/(hr)(ft^2)($^\circ$F)), an average thermal-layer thickness is $\delta \approx 0.017$ inch.

The relation of Han and Griffith (ref. 4) as given in equation (2) is plotted in figure 3(a) using the thermal-layer thickness of 0.017 inch, and it appears to bound most

of the data. A detailed examination of the agreement with the data, however, reveals some important discrepancies. For the saturated case, the maximum value of equation (2), which is found as $(\Delta T)_i \to \infty$, is $R_{c,max} = 2\delta/3 = 0.011$ inch. The theory does not account for the observed activity of the largest drilled sites used here which had $R_c = 0.032$ inch. Possibly even larger sites would produce bubbles, so the data do not confirm the theoretical prediction that there is a maximum cavity radius that is active. Although the theoretical curve does encompass much of the data, it does not really pass through the lower bounds of the experimental $(\Delta T)_i$ points; rather it predicts $(\Delta T)_i$ values that are generally much too low. This type of comparison between data and theory is also evident for the measurements reported in reference 11.

In addition to requiring a value of δ, equation (3) of Hsu (ref. 3) has coefficients C_1 and C_3 that depend on the cavity geometry. If the values of C_1 and C_3 used in reference 3 are assumed here, a curve similar to that from equation (2) is obtained. If as an extreme case the mouth of the cavity is assumed to have a perfectly square edge which would be approached by the machine drilled sites, then from the results of reference 3 it can be shown that C_1 and C_3 are equal to one. With these values, equation (3) was evaluated and is shown in figures 3(a) and (b). The curve, which strictly should be compared only with the mechanically drilled data because of the choice of constants, encompasses a little higher range of cavity radii than the Han and Griffith relation, but it still does not bound the data for the largest sites studied here.

It could be argued that the nucleation that appears to come from the large cavities is occurring at smaller nucleation sites contained within the larger sites. However, Bankoff (ref. 12) shows that rectangular grooves up to a width of 0.07 centimeter (0.028 in.) will retain any vapor originally trapped within them when immersed. He further states that a cylindrical cavity of this ($R_c = 0.014$ in.) or somewhat larger radius should also retain entrapped vapor. The high-speed motion pictures, discussed in succeeding sections, showed a vapor cap left over the site by each departing bubble. Hence, it appears that the prepared sites remained filled with vapor, which makes the "site within a site" explanation doubtful. The fact that the nucleus over a large nucleation site was found to grow in a saturated liquid indicates that the maximum critical cavity radius predicted by the analyses of references 3 and 4 may be unrealistic at least for the saturated case.

The activation theories were founded on the assumption that for a bubble to begin to grow, the temperature in the thermal layer at a characteristic position, for example, at the top of the bubble nucleus, must reach the temperature of the vapor inside the nucleus. More realistically the growth would seem to depend on whether there is a net vapor addition to the bubble which in turn depends on a net heat addition to the bubble. If a bubble nucleus extends out beyond the thermal layer, the theory in references 3 and 4 would predict the site to be inactive. However, the present authors believe that

if there is sufficient heat addition to the bubble nucleus in the region near its base, the nucleus may still grow even though it extends beyond the thermal layer.

The present authors have devised a cavity activation criterion based on a heat balance to the bubble nucleus, and the analysis is given in appendix B. Although forming a heat balance appears to be a reasonable approach, the predictions were not much more successful than the previous analyses mentioned. As shown in figure 3(b), the results were close to those of equation (4) and provided values of $(\Delta T)_i$ that were too small. The analysis is included in this report for possible interest to those who may perform further investigations in this area.

A summarization is as follows: Values of $(\Delta T)_i$ to initiate bubble production have been determined experimentally for a range of cavity radii and have been compared with theoretical predictions of cavity activation. The presently available analyses do not seem satisfactory for predicting the experimental observations. The observed $(\Delta T)_i$ were always significantly higher than those predicted.

Characteristics of Bubbles at Drilled Sites

Growth of bubbles while attached to surface. - If mechanically drilled sites in a polished surface and low heat fluxes near incipience were used, it was possible to grow isolated bubbles which were not disturbed by any adjacent bubble formation. The high-speed motion pictures showed the bubble profiles to be symmetric about the site axis, and the bubbles had little distortion. Figures 4(a) and (b) show a set of tracings for the growth of two bubbles, one for each of the mechanically drilled site diameters 0.0075 and 0.0413 inch. These sites along with two other sites were drilled into the same heated strip, and the photographs were taken at the four sites in rapid succession without changing the experimental conditions; thus, the heat flux and the surface temperature were held constant. Hence, the pictures presumably compare the growth of bubbles under the same condition of the thermal layer on the surface. The random convective circulation currents in the boiler, however, caused, some fluctuations in the thermal layer thickness. These fluctuations resulted in some of the bubbles at a given site having lower growth rates than others even though the time average conditions remained fixed. This statistical variation was also noted in reference 9. The statistical randomness must be removed as much as possible in order to help provide a consistent comparison of bubbles taken at different sites. The minimization of randomness was done by selecting the bubble at each site that had the most rapid growth rate and increased in volume continuously to detach in the shortest growth period. The conditions for the growth of such bubbles should correspond most closely to the conditions for which the theoretical growth equations apply. These are the bubbles shown for two of the sites in

figure 4 and are presumed to be growing under thermal conditions as consistent with each other as possible. The surface- to bulk-temperature difference was 12.5° F.

The bubbles were assumed to be rotationally symmetric about each site axis, and their volumes were computed from the profiles. For some of the bubbles near detachment, where they were not close to spherical, the width of the bubble was measured at 15 positions along the bubble height, and the volume was computed by numerical integration. For the remainder of the bubbles, the shape could be approximated within an error of a few percent by a sphere or a spherical segment, and the volume computed by using spherical volume formulae.

The volumes are given as a function of time in figure 5 for the entire growth period. Since the photographs were taken at a film speed of approximately 2000 frames per second, there is a time lapse of somewhat less than 1/2000 second between frames as recording the image on the film requires a portion of the time. Hence, the first datum point can be, at most, a few ten thousandths of a second after the detachment of the previous bubble. If the data could be extrapolated to zero time, the initial bubble volume would not be zero because there was always a vapor nucleus left behind by the previous bubble. The last few pictures in each set of bubble profiles in figure 4 illustrate how the bubble neck narrows and then breaks off thereby leaving a vapor nucleus behind.

The present data are compared in figure 5 with two of the commonly quoted simple equations for bubble growth: the Fritz-Ende expression (ref. 16)

$$V = \frac{\pi}{6}\left(\frac{4k_l \Delta T}{\lambda \rho_v}\right)^3 \left(\frac{\tau}{\pi \alpha}\right)^{3/2} \tag{5}$$

and the Plessett-Zwick expression (ref. 17)

$$V = \frac{\pi\sqrt{3}}{2}\left(\frac{4k_l \Delta T}{\lambda \rho_v}\right)^3 \left(\frac{\tau}{\pi \alpha}\right)^{3/2} \tag{6}$$

These expressions do not fit the slope of the data over the entire growth period, as the observed bubbles do not have a $V \propto \tau^{3/2}$ variation throughout growth. The Fritz-Ende result, which is based on a less refined conduction model than the Plessett-Zwick equation, agrees more closely with the range of data although the theory predicts a more rapid growth than that observed. The better agreement of the Fritz-Ende relation with the measured growth data was also found for the data in reference 18.

In figure 6(a), the growth curves of bubbles from an artificial site of diameter $D_c = 0.0075$ inch are shown as a function of the surface- to bulk-temperature difference.

The curves shown were selected, as in figure 5, as being the ones which had the most rapid bubble growth. It was felt that these curves should correspond most closely with the the analytical predictions, as they presumably are for very favorable growth conditions. Comparison is made with the Fritz-Ende equation, and, although the experimental data do not fall on the analytical lines, agreement insofar as trends with ΔT and slopes with time is good. As shown by equations (5) and (6), the bubble volume should depend on $(\Delta T)^3$, and this relation is indicated to some extent by comparing the data of figure 6(a) to the curves of the Fritz-Ende relation. The variation of volume with ΔT will be discussed in more detail in connection with figure 7.

In figure 6(b), growth curves for bubbles originating at a larger site with diameter $D_c = 0.0413$ inch are shown. The correlation with the analytical curves, and the self-consistency of the data is obviously poorer than for the smaller site. Two possible reasons for poorer correlation are evident. First, the models used in deriving the analytical expressions have the assumption that the bubble is surrounded by superheated liquid. This assumption is of doubtful validity for the very large bubbles growing from the larger sites especially during the later stages of growth. Also, because of the lower frequency of bubble emission from the larger sites at a given ΔT, relatively fewer bubbles were available on each film roll for obtaining growth curves. Thus, in selecting the most rapid growth curve for each given ΔT, the probability of obtaining comparable curves for comparison between the different ΔT values was not as good as for the higher frequency small site.

In figure 7, the growth data of figure 6(a) for bubbles nucleated from the 0.0075-inch diameter site are cross-plotted to show more clearly the relation between bubble volume and ΔT at fixed times from the beginning of bubble growth. The increase in bubble volume with $(\Delta T)^3$ as predicted by the Fritz-Ende equation is shown by the dotted lines, and agreement with the limited data available seems reasonable.

Interpretation of bubble-growth results. - Some aspects of bubble departure from a known site have been studied previously by Wei and Preckshot (ref. 19), who photographed bubbles leaving a short section of glass capillary that had been cemented to a glass slide placed on a heated copper block. The entire assembly was submerged in water and bubbles nucleated from the capillary. In this case, where the cavity itself was not within the heat generating material, after a bubble detached there was a small vapor pocket left at the bottom of the cavity, and the remainder of the cavity filled with liquid. The small vapor pocket grew to form the next bubble. In the present experiments, the cavity was drilled into the heat generating material of the test strip, and either because of this or the cavity shape or material, the vapor nucleus was much larger than that in reference 19. The vapor nucleus was always observed to protrude well above the cavity opening. For this reason, it is possible that the walls within the cavity were dry without any liquid layer penetrating inside. Within the very short time

after bubble departure and before the next frame showing the new bubble, the surface tension formed the nucleus into the shape of a spherical surface. For a small site (fig. 4(a)), the nucleus was almost in the shape of a complete sphere, while for a larger site (fig. 4(b)), it was approximately a spherical segment.

It is postulated herein as a possible growth mechanism that the growth of the bubble depends on the heat addition from the thermal layer at the bubble base. Hence, the growth of the bubble depends on how much surface area it has within the thermal layer. Analyses such as those by Zuber (ref. 20) and Han and Griffith (ref. 4) assume that the growing bubble nucleus pushes the thermal layer outward; thus the bubble is surrounded by the thermal layer. As was discussed in the section Growth of Bubbles While Attached to Surface, the thermal-layer thickness for the heat fluxes encountered here was on the order of 0.017 inch in thickness. This thickness is shown in figure 4 and is a little larger than the height of the vapor nucleus left behind by the departing bubble. During most of the bubble-growth period, the thermal layer was small compared with the bubble height. This comparison was true for the cases reported herein because the artificial sites were fairly large, and large bubbles were produced. As a result, it is possible that the heat transfer to a bubble was only through the area of the base in contact with the thermal layer. This area is identified as the area A in figure 8. The growth of the bubble then depends on the time variation of A. As a very simple illustration, assume that the heat-transfer coefficient at the bubble base and the average temperature within the thermal layer remain constant throughout bubble growth. Then, the energy added from the liquid to the bubble is equated to the energy required to provide vapor for bubble growth:

$$hA(T_{t\ell} - T_v) = \frac{dV}{d\tau}\rho_v\lambda \tag{7}$$

The time variation of A then must be considered in order to integrate for V. From the bubble profiles in figure 4, after about the first 0.001 second the bubbles are quite close to spherical segments and are of the successive configurations shown in figure 8(b). The area A of any spherical zone is given by πDL, where L is the height of the zone. Therefore, the area of the spherical zone within the thermal layer is $A = \pi D\delta$. If the volume of the bubble is approximated by $V = \pi D^3/6$, then $A = \pi(6V/\pi)^{1/3}\delta$. Substituting into equation (7) and assuming that the thermal-layer temperature and thickness remain constant during bubble growth give the functional form

$$V^{1/3} \propto \frac{dV}{d\tau}$$

or

$$V \propto \tau^{3/2} \tag{8}$$

In the later stages of growth when the bubble begins to elongate and especially when a neck begins to form, the area A tends to become constant, especially for the bubbles from large sites as in figure 8(c). Then from equation (7), $dV/d\tau$ = constant, which gives

$$V \propto \tau \tag{9}$$

This first power behavior of the volume with time was also observed in reference 18. The trend of decreasing slope during growth of the curves in figures 5 and 6 then might be attributed in part to the changing configuration near the bubble base. The fact that the temperature in the thermal layer T_{tl} actually decreases during growth (refs. 21 and 22) and that the heat added from the thermal-layer thickness δ may also decrease during growth (ref. 23) contributes further to a reduction in growth rate.

When a bubble is formed at a very small natural nucleation site, the edge of the bubble base grows beyond the limits of the site opening. The base expands rapidly outward at first, and then the base diameter remains relatively constant until bubble detachment begins (e.g., base-diameter measurements in ref. 18). The rapid growth in the base diameter produces a rapid increase in the bubble area within the thermal layer which could account for the fact that in the expression (ref. 24)

$$D \propto \tau^{n} \tag{10}$$

the n values have been as large as one near the beginning of bubble growth.

Forces acting on bubbles at departure. - The shapes of typical bubbles formed at drilled sites are shown in figure 9 just prior to the beginning of necking at the base of the bubble, which is the start of bubble departure. In the present experiments, the forces on the bubble at departure are believed to be computed very accurately because of the following considerations: At departure, the cylindrical neck at the base of the bubble was found to stretch in length and become narrower until the neck was broken. Hence, the force holding the bubble to the surface is the surface tension of the interface around the circumference of the bubble neck. Consequently, for the bubbles considered herein, the surface-tension force can be computed quite accurately since it does not depend on the contact angle where the liquid-vapor interface meets the heated surface. During boiling, this contact angle is difficult to measure experimentally with high accuracy. As will be shown, the diameter of the bubble neck is known accurately here

because it corresponds quite well with the diameter of the drilled site.

The buoyancy force of the bubble at departure can be computed by a method proposed in reference 25. The bubble parameters that were obtained from the photographs are the total volume V, horizontal maximum diameter D, height H, and base diameter D_b as shown in figure 9(d). The buoyancy expression will be placed in terms of these quantities. The buoyancy of the bubble volume, excluding the shaded volume V_b of figure 9(d), is given by

$$(\rho_l - \rho_v) \frac{g}{g_o} (V - V_b)$$

Assume the shaded volume is approximated closely by a cylinder (thus, neglect the curvature of the top of the bubble); this term can then be written as

$$(\rho_l - \rho_v) \frac{g}{g_o} \left(V - \frac{\pi D_b^2 H}{4} \right) \tag{11}$$

The contribution of V_b to the buoyancy force can be expressed in terms of the pressure difference across the interface at the top of the bubble

$$\frac{\pi D_b^2}{4} (P_v - P_o) \tag{12}$$

This pressure difference can be written in terms of the two principal radii of curvature at the top of the bubble

$$(P_v - P_o) = \sigma \left(\frac{1}{R_1} + \frac{1}{R_2} \right)_{\text{top of bubble}} \tag{13}$$

For the bubbles given herein, the upper portions are so spherical that R_1 and R_2 at the top of the bubble can both be approximated by $R_1 = R_2 = D/2$. The sum of equations (11) and (12) with the use of equation (13) provides the final expression used to compute the buoyant departure force.

$$F_B = (\rho_l - \rho_v) \frac{g}{g_o} \left(V - \frac{\pi D_b^2 H}{4} \right) + \frac{\pi D_b^2 \sigma}{D} \tag{14}$$

As discussed earlier, the bubble departs by breaking the neck a little above the position where it is in contact with the surface. The surface-tension force is then given by

$$F_T = \sigma \pi D_b \tag{15}$$

The width of the neck at the bubble base was measured from the photographs. As shown by the values in figure 9, the width was found to be quite close to the diameter of the drilled site except for the smallest site photographed where in one instance the neck appeared somewhat wider than the site. Since the drilled holes were measured directly with a microscope, the precision is higher than the photographic measurement at the bubble base as the photographs are distorted somewhat by density gradients in the fluid. Hence, using the diameter of the drilled site and computing the surface tension force from

$$F_T = \sigma \pi D_c \tag{16}$$

is considered more accurate. As shown in the previous section on bubble growth rates, the volume change with time for the present bubbles was small at the time of departure. This small growth rate eliminates the possibility of inertial forces being of significance. It also eliminates the consideration of drag forces resulting from the motion of the expanding surface of the bubble.

A summary of bubble-departure dimensions and forces is given in table II. A plot of buoyancy against surface-tension force is given in figure 10. Within a statistical scatter that seems reasonable for a boiling experiment, the agreement of the two forces is very good. This agreement shows that for the large slowly growing bubbles studied herein, the buoyancy force defined as the integrated vertical pressure force on the bubble is the force causing departure.

Equilibrium bubble shapes. - In reference 26, Bashforth and Adams studied the shapes of drops and bubbles at equilibrium subject to the forces of buoyancy and surface tension. They provide tables of coordinates of the bubble profiles in terms of the parameter

$$\beta = \frac{g(\rho_v - \rho_l)b^2}{g_o \sigma}$$

Since some of the present bubbles fall so close to the correlating line in figure 10, which indicates an equilibrium between surface tension and buoyancy forces at departure, it is

of interest to see whether these bubbles compare with the predicted equilibrium shapes. Only the shapes are being compared and not the actual bubble sizes since the theoretical results are in terms of dimensionless heights and radii utilizing the radius of curvature b at the top of the bubble as a scale factor. Multiplying by the dimension b to place the curves in dimensional form would not change the relative shapes at a fixed β. Since ρ_l is greater than ρ_v, the values of β are negative for the present results. The two typical experimental bubbles shown in figure 11 have values of $\beta = -0.24$ and -0.35 and grew at mechanically drilled site diameters of 0.0209 and 0.0413 inch, respectively. The tables of bubble coordinates in reference 26 are somewhat incomplete in the range of $\beta = -0.1$ to -0.3, and the theoretical curves were supplemented with values given in reference 27.

The comparisons in figure 11 reveal that the upper portions of the experimental bubbles are very close to spherical and agree well with the theory. At the base portion of the bubbles, the experimental profiles deviate from theory probably because of the physical constraint imposed by the attachment of the bubble base to the opening of the drilled site. The theory on the other hand does not have this constraint. These considerations reveal an additional factor, other than dynamic forces present for rapidly growing bubbles, which would account for why the Fritz equation (ref. 28) does not always correctly predict the size of bubbles at departure. The Fritz equation is based on theory which assumes that the base of the bubble is not constrained while, depending on the site diameter and geometry, the base of some actual boiling bubbles can remain attached to the site as in the present study.

CONCLUSIONS

1. Bubble incipience is a vague concept in relation to interpretation of experimental data. Analytical determinations of site activation consider the surface superheat required to make a bubble nucleus grow although the bubble may not then detach. Incipience is defined here in terms of the condition when a steady bubble stream is being formed. This condition requires that the bubble must not only begin to grow, but it must also be able to reach a size sufficient to cause detachment.

2. Experimental values were obtained for the surface superheat when a cavity begins to produce bubbles, and the results were compared with several analyses. For the range of cavity radii tested, 0.0015 to 0.032 inch, the predicted $(\Delta T)_i$ were always significantly smaller than those measured.

3. The experimental results show that there can be active cavities which are larger than those indicated by some of the analytical models relating cavity size and thermal-layer thickness for site activation. These models predict that the maximum active site

radius is comparable to the thermal-layer thickness, whereas experimentally much larger sites were found active. This conclusion is based on the assumption that a thermal layer of thickness 0.017 inch is present in the present experiments. The upper limit of active site radius is probably governed in part by the ability of liquid to fill the site rather than by considerations of thermal effects.

4. In the initial period of bubble growth, the bubble volume was found proportional to $(\text{time})^{3/2}$. Later in the growth period, the volume is proportional to time, which implies that vapor addition to the bubble may take place through a constant area around the bubble neck.

5. For a given small site, the volumetric growth rate increases approximately as $(\Delta T)^3$ as indicated by many of the growth equations, where ΔT is the difference between the temperature at the boiling surface and the saturation temperature. For a large site, the functional relation is not clear, but the growth rate does increase with ΔT.

6. The bubbles detach from the artificial sites studied here by forming a neck which is ruptured some distance above the site. Consequently, a vapor nucleus is left behind from which the next bubble grows.

7. For slowly growing bubbles, the buoyancy and surface-tension forces are in balance at bubble detachment. The buoyancy force must include the pressure force deficit caused by the missing bubble surface area in the contact region at the bubble base.

8. Although uniform temperature conditions were not present, the bubbles near their departure from the artificial sites compared reasonably well with the equilibrium shapes predicted by Bashforth and Adams. Near the bubble base, the constraint imposed by attachment to the artificial site causes some deviation from the predicted shapes.

Lewis Research Center,
National Aeronautics and Space Administration,
Cleveland, Ohio, February 13, 1967,
129-01-11-06-22.

APPENDIX A

SYMBOLS

A	surface area
a	thickness of specimen containing artificial site
b	radius of curvature at top of bubble
C_1, C_3	dimensionless site geometry constants
D	maximum horizontal bubble diameter
D_b	base diameter of bubble
D_c	diameter of artificial nucleation cavity
F_B	buoyancy force
F_T	surface-tension force
g	gravitational acceleration
g_o	conversion constant, 32.2 lb-mass-ft/lb force-sec^2
H	bubble height
h	boiling heat-transfer coefficient
h_e, h_c	evaporating and condensing heat-transfer coefficients for heat transfer to bubble nucleus
k, k_l	thermal conductivity of test specimen or liquid
P_v, P_o	internal and external pressure at top of bubble
Q	energy per unit time
q	heat flux
R	bubble radius
R_c	radius of artificial nucleation cavity
R_1, R_2	principal radii of curvature of bubble
ΔT	temperature difference, $T_w - T_{sat}$
T_{bulk}	bulk temperature of boiling liquid
T_o	temperature at insulated surface of test specimen
T_{sat}	saturation temperature of boiling liquid
T_{tl}	mean thermal-layer temperature
T_v	temperature of vapor inside bubble
T_w	temperature of boiling surface of test specimen
V	volume of bubble
V_b	bubble volume which lies above area of bubble base
x	distance coordinate from surface
α	thermal diffusivity
β	bubble-shape parameter, $\frac{g}{g_o}\frac{(\rho_v - \rho_l)b^2}{\sigma}$
δ	thermal-layer thickness
λ	heat of vaporization

ρ_l, ρ_v	density of liquid or vapor
σ	surface tension of liquid-vapor interface
τ	time

Subscripts:

bulk	fluid bulk condition
i	condition at incipience
sat	saturated
v	vapor

APPENDIX B

CAVITY ACTIVATION CRITERION

The analysis presented herein is based on an energy balance for a bubble nucleus that is assumed to exist at a nucleation site. As discussed in reference 5, as a vapor nucleus grows out of a surface cavity, the minimum radius of curvature of the vapor-liquid interface is reached when the vapor cap becomes a hemisphere. The hemispherical nucleus will be the most difficult bubble configuration to grow and will thus have the highest vapor temperature within it. For this reason, the analysis will deal with the growth of a hemispherical nucleus. This nucleus is represented in figure 12. Although the data in the present report are for saturated bulk liquid, the analysis will include the subcooled case.

Temperature Profile

As shown in figure 13, for simplicity the temperature distribution in the liquid thermal layer near the surface will be approximated by a straight line extending from the wall to the thickness δ_{bulk} where the bulk temperature is reached. The thickness δ designates the position at which the fluid is at the saturation temperature. The temperature profile is then given as

$$T(x) = T_{bulk} + (T_w - T_{bulk})\left(1 - \frac{x}{\delta_{bulk}}\right) \qquad x \leq \delta_{bulk} \tag{B1}$$

$$T(x) = T_{bulk} \qquad x \geq \delta_{bulk} \tag{B2}$$

Growth Criteria for Bubble Nucleus

A hemispherical vapor nucleus is now assumed to be on the surface cavity. This assumption is somewhat restrictive since for high subcooling, especially in conjunction with a large cavity size, the nucleus may not be able to grow this large. The vapor temperature within the nucleus is assumed to be constant and is given by (ref. 5)

$$T_v - T_{sat} = \frac{2\sigma T_{sat}}{\lambda \rho_v R_c} \tag{B3}$$

Three cases can be distinquished depending on the relation of cavity radius to the thermal-layer thickness. One case is shown in figure 12(a) where the nucleus extends through the thermal layer ($R_c \geq \delta_{bulk}$). Figure 12(b) where $R_c \leq \delta_{bulk}$ provides the other two cases depending on the size of R_c relative to δ_v, the position at which $T(x) = T_v$. The two cases are thus for $\delta_{bulk} \geq R_c \geq \delta_v$ and for $0 \leq R_c < \delta_v$. If equation (B3) is used for the vapor temperature within the bubble, the net heat addition to the nucleus is

$$Q = h_e 2\pi R_c \int_0^{\delta_v} \left[T_{bulk} + (T_w - T_{bulk})\left(1 - \frac{x}{\delta_{bulk}}\right) - T_{sat} - \frac{2\sigma T_{sat}}{\lambda \rho_v R_c} \right] dx$$

$$+ h_c 2\pi R_c \int_{\delta_v}^{\delta_{bulk}} \left[T_{bulk} + (T_w - T_{bulk})\left(1 - \frac{x}{\delta_{bulk}}\right) - T_{sat} - \frac{2\sigma T_{sat}}{\lambda \rho_v R_c} \right] dx$$

$$+ h_c 2\pi R_c \int_{\delta_{bulk}}^{R_c} \left(T_{bulk} - T_{sat} - \frac{2\sigma T_{sat}}{\lambda \rho_v R_c} \right) dx \qquad R_c \geq \delta_{bulk} \qquad \text{(B4a)}$$

$$Q = h_e 2\pi R_c \int_0^{\delta_v} \left[T_{bulk} + (T_w - T_{bulk})\left(1 - \frac{x}{\delta_{bulk}}\right) - T_{sat} - \frac{2\sigma T_{sat}}{\lambda \rho_v R_c} \right] dx$$

$$+ h_c 2\pi R_c \int_{\delta_v}^{R_c} \left[T_{bulk} + (T_w - T_{bulk})\left(1 - \frac{x}{\delta_{bulk}}\right) - T_{sat} - \frac{2\sigma T_{sat}}{\lambda \rho_v R_c} \right] dx \qquad \delta_{bulk} \geq R_c \geq \delta_v \qquad \text{(B4b)}$$

$$Q = h_e 2\pi R_c \int_0^{R_c} \left[T_{bulk} + (T_w - T_{bulk})\left(1 - \frac{x}{\delta_{bulk}}\right) - T_{sat} - \frac{2\sigma T_{sat}}{\lambda \rho_v R_c} \right] dx \qquad 0 \leq R_c \leq \delta_v$$

(B4c)

The quantities h_e and h_c are the evaporating and condensing heat-transfer coefficients for heat transfer to the nucleus and have been assumed constant. For the nucleus to grow, Q must be greater than zero. Solving equations (B4) for the activation criterion $Q \geq 0$ and assuming $h_c = h_e$ result in the following two relations

$$\left(T_w - T_{sat}\right)_i = (\Delta T)_i \geq \frac{4\sigma T_{sat}}{\lambda \rho_v \delta_{bulk}} + (T_{sat} - T_{bulk})\left(\frac{2R_c}{\delta_{bulk}} - 1\right) \qquad R_c \geq \delta_{bulk} \quad \text{(B5a)}$$

$$(\Delta T)_i \geq \frac{2\sigma T_{sat}}{\lambda \rho_v R_c \left(1 - \frac{R_c}{2\delta_{bulk}}\right)} + \frac{(T_{sat} - T_{bulk})\frac{R_c}{2\delta_{bulk}}}{1 - \frac{R_c}{2\delta_{bulk}}} \qquad R_c \leq \delta_{bulk} \quad \text{(B5b)}$$

Equation (B5b) incorporates the incipience criterion for both (B4b) and (B4c). For saturated conditions $T_{bulk} = T_{sat}$ and $\delta_{bulk} = \delta$, equations (B5a) and (B5b) become

$$(\Delta T)_{i,\,sat} \geq \frac{4\sigma T_{sat}}{\lambda \rho_v \delta} \qquad R_c \geq \delta \quad \text{(B6a)}$$

$$(\Delta T)_{i,\,sat} \geq \frac{2\sigma T_{sat}}{\lambda \rho_v R_c \left(1 - \frac{R_c}{2\delta}\right)} \qquad R_c \leq \delta \quad \text{(B6b)}$$

When equations (B5a) and (B5b) are compared with equations (B6a) and (B6b) it is evident that relative to the saturated condition the subcooling provides an additional term that increases the temperature difference required for growth of the nucleus. No maximum site radius that will be active is indicated by this analysis.

A similar analysis except that it is based on the surface heat flux rather than the surface temperature has been given by Grace (ref. 29).

Temperature Difference Required for Bubble Detachment

For a saturated bulk fluid, if the activation ΔT is exceeded, the theory predicts that bubbles will grow until they detach from the surface. When the bulk is subcooled, however, the upper portion of the bubble may protrude into liquid that is below the vapor

temperature within the bubble, and condensation will occur. As a bubble grows, a size may be reached where the condensation balances the evaporation in the region near the bubble base. Then the bubble can no longer increase in size. If this zero net heat addition condition occurs before the bubble has reached the size necessary for detachment, the bubble will not leave the surface. Then the site is not incipient because no stream of bubbles is being produced. Thus, in the case of a subcooled fluid, two criteria have to be examined with regard to the definition of incipience. The first is whether a vapor nucleus at the nucleation site will grow; the second is whether a bubble can become large enough to detach from the surface and produce a stream of bubbles.

To arrive at a criterion for whether bubbles will grow to detachment, the size a bubble will achieve must be expressed in terms of the subcooling. For simplicity, the bubble is assumed to be a portion of a sphere as shown in figure 14. The bubble radius, height, and the cavity radius are then related by

$$R = \frac{H^2 + R_c^2}{2H} \tag{B7}$$

The final expressions may be simplified by the assumption that the evaporation and the condensation heat-transfer coefficients are equal. Then the heat addition to the bubble is

$$Q = 2\pi R h_e \left\{ \int_0^{\delta_{bulk}} \left[(T_w - T_{bulk}) \left(1 - \frac{x}{\delta_{bulk}} \right) + T_{bulk} - T_{sat} - \frac{2\sigma T_{sat}}{\lambda \rho_v R} \right] dx \right.$$

$$\left. + \int_{\delta_{bulk}}^{H} \left(T_{bulk} - T_{sat} - \frac{2\sigma T_{sat}}{\lambda \rho_v R} \right) dx \right\} \qquad H \geq \delta_{bulk} \tag{B8a}$$

$$Q = 2\pi R h_e \int_0^{H} \left[(T_w - T_{bulk}) \left(1 - \frac{x}{\delta_{bulk}} \right) \right.$$

$$\left. + T_{bulk} - T_{sat} - \frac{2\sigma T_{sat}}{\lambda \rho_v R} \right] dx \qquad H \leq \delta_{bulk} \tag{B8b}$$

The heat addition Q is set equal to zero to provide the condition when the bubble will remain of fixed size. The integrals are carried out, and the radius R is eliminated in

terms of the height H by using equation (B7). The result is an implicit expression for the height of the equilibrium bubble,

$$\frac{H}{\delta_{bulk}} = \frac{1}{2}\left(\frac{T_w - T_{sat}}{T_{sat} - T_{bulk}} + 1\right) - \frac{4\sigma T_{sat}}{\lambda\rho_v\delta_{bulk}(T_{sat} - T_{bulk})}\frac{H^2}{H^2 + R_c^2} \qquad H \geq \delta_{bulk} \qquad \text{(B9a)}$$

$$\frac{H}{\delta_{bulk}} = \frac{2(T_w - T_{sat})}{(T_w - T_{sat}) + (T_{sat} - T_{bulk})}$$

$$- \frac{8\sigma T_{sat}}{\lambda\rho_v\left[(T_w - T_{sat}) + (T_{sat} - T_{bulk})\right]}\frac{H}{\left(H^2 + R_c^2\right)} \qquad H \leq \delta_{bulk} \qquad \text{(B9b)}$$

If a given set of variables such as subcooling, cavity radius, etc., is inserted into equation (B9), the equilibrium bubble height can be found, and the question then remains as to whether a bubble of this height will depart from the surface.

The departure depends on the balance of forces on the bubble. The most simple case, which was valid for the large sites in saturated liquid studied herein, is when the departure depends only on the balance of buoyancy and surface tension. By equating equations (14) and (16), the bubble height at departure is obtained in terms of the cavity radius. The height can then be compared with that from equation (B9) to determine whether departure will occur.

REFERENCES

1. Zuber, Novak: Recent Trends in Boiling Heat Transfer Research. Part I: Nucleate Pool Boiling. Appl. Mech. Rev., vol. 17, no. 9, Sept. 1964, pp. 663-672.

2. Leppert, G.; and Pitts, C. C.: Boiling. Advances in Heat Transfer, Vol. 1, Thomas F. Irvine, Jr. and James P. Hartnett, eds., Academic Press, 1964, pp. 185-266.

3. Hsu, Y. Y.: On the Size Range of Active Nucleation Cavities on a Heating Surface. J. Heat Transfer, vol. 84, no. 3, Aug. 1962, pp. 207-216.

4. Han, Chi-Yeh; and Griffith, Peter: The Mechanism of Heat Transfer in Nucleate Pool Boiling. Part I. Bubble Initiation, Growth, and Departure. Int. J. Heat Mass Transfer, vol. 8, no. 6, June 1965, pp. 887-904.

5. Griffith, P.; and Wallis, J. D.: The Role of Surface Conditions in Nucleate Boiling. AIChE Chem. Engr. Progr. Symp. Ser., vol. 56, no. 30, 1960, pp. 49-63.

6. Madejski, J.: Activation of Nucleation Cavities on a Heating Surface With Temperature Gradient in Superheated Liquid. Int. J. Heat Mass Transfer, vol. 9, no. 4, Apr. 1966, pp. 295-300.

7. Leont'ev, A. I.; and Kirdyashkin, A. G.: The Theory of the Convective Heat Transfer for the Vertical Flow of Fluid. Proceedings of the Third International Heat Transfer Conference, Chicago, Aug. 8-12, 1966, ASME-AIChE, 1966, vol. I, pp. 216-224.

8. Rallis, C. J.; and Jawurek, H. H.: The Mechanism of Nucleate Boiling. Reactor Engineering and Equipment. Vol. 8 of the Proceedings of the Third International Conference on the Peaceful Uses of Atomic Energy, Geneva, Aug. 31-Sept. 9, 1964. United Nations, 1965, pp. 156-165.

9. Strenge, P. H.; Orell, Aluf; and Westwater, J. W.: Microscopic Study of Bubble Growth During Nucleate Boiling. AIChE J. vol. 7, no. 4, Dec. 1961, pp. 578-583.

10. Yatabe, J. M.; and Westwater, J. W.: Bubble Growth Rates for Ethanol-Water and Ethanol-Isopropanol Mixtures. AIChE Paper no. 7, presented at the ASME-AIChE 8th National Heat Transfer Conference, Los Angeles, Aug. 1965.

11. Hatton, A. P.; and Hall, I. S.: Photographic Study of Boiling on Prepared Surfaces. Proceedings of the Third International Heat Transfer Conferenee, Chicago, Aug. 8-12, 1966, ASME-AIChE, 1966, vol. 4, pp. 24-37.

12. Bankoff, S. G.: Entrapment of Gas in the Spreading of a Liquid Over a Rough Surface. AIChE J., vol. 4, no. 1, Mar. 1958, pp. 24-26.

13. Howell, J. R.; and Siegel, R.: Incipience, Growth, and Detachment of Boiling Bubbles in Saturated Water from Artificial Nucleation Sites of Known Geometry and Size. Proceedings of the Third International Heat Transfer Conference, Chicago, Aug. 8-12, 1966, ASME-AIChE, 1966, vol. 4, pp. 12-23.

14. Jeglic, Frank, A: An Analytical Determination of Temperature Oscillations in a Wall Heated by Alternating Current. NASA TN D-1286, 1962.

15. Marcus, B. D.; and Dropkin, D.: Measured Temperature Profiles Within the Superheated Boundary Layer Above a Horizontal Surface in Saturated Nucleate Pool Boiling of Water. J. Heat Transfer, vol. 87, no. 3, Aug. 1965, pp. 333-341.

16. Fritz, W.; and Ende, W.: The Vaporization Process According to Cinematographic Pictures of Vapor Bubbles. Physik. Z., vol. 37, 1936, pp. 391-401.

17. Plesset, M. S.; and Zwick, S. A.: The Growth of Vapor Bubbles in Superheated Liquids. J. Appl. Phys., vol. 25, no. 4, Apr. 1954, pp. 493-500.

18. Siegel, R.; and Keshock, E. G.: Effects of Reduced Gravity on Nucleate Boiling Bubble Dynamics in Saturated Water. AIChE J., vol. 10, no. 4, July 1964, pp. 509-517.

19. Wei, Ching-Chen; and Preckshot, G. W.: Photographic Evidence of Bubble Departure from Capillaries During Boiling. Chem. Eng. Sci., vol. 19, no. 10, Oct. 1964, pp. 838-839.

20. Zuber, Novak: The Dynamics of Vapor Bubbles in Nonuniform Temperature Fields. Int. J. Heat Mass Transfer, vol. 2, no. 1/2, 1961, pp. 83-98.

21. Moore, Franklin D.; and Mesler, Russell B.: The Measurement of Rapid Surface Temperature Fluctuations During Nucleate Boiling of Water. AIChE J., vol. 7, no. 4, Dec. 1961, pp. 620-624.

22. Morin, René: Fundamental Studies in Boiling. Proceedings of the 2nd Joint USAEC-Euratom Two-Phase Flow Meeting, Germantown, Maryland, Apr. 29-May 1, 1964. AEC, 1964, pp. 15-16.

23. Hsu, Yih-Yun; and Graham, Robert W.: An Analytical and Experimental Study of the Thermal Boundary Layer and Ebullition Cycle in Nucleate Boiling. NASA TN D-594, 1961.

24. Staniszewski, Bogurmil, E.: Nucleate Boiling Bubble Growth and Departure. Tech. Rep. No. 16, Massachusetts Inst. Tech., Aug. 1959.

25. Cochran, Thomas H.; and Aydelott, John C.: Effects of Subcooling and Gravity Level on Boiling in the Discrete Bubble Region. NASA TN D-3449, 1966.

26. Bashforth, Francis; and Adams, J. C.: An Attempt to Test the Theories of Capillary Action by Comparing the Theoretical and Measured Forms of Drops of Fluid. Cambridge University Press, 1883.

27. Chun, Ke-Sang: A Study of Steam Bubbles in Nucleate Boiling. PhD Thesis, Illinois Inst. Tech., 1956.

28. Fritz, W.: Maximum Volume of Vapour Bubbles. Phys. Zeits., vol. 36, June 1, 1935, pp. 379-384.

29. Grace, Thomas M.: The Mechanism of Burnout in Initially Sub-Cooled Forced Convective Systems. PhD Thesis, University of Minnesota, 1964.

TABLE I. - TEMPERATURE DIFFERENCE BETWEEN SURFACE AND SATURATED LIQUID FOR STEADY BUBBLE PRODUCTION, SATURATED CONDITIONS

Electron-beam drilled sites		Machine drilled sites		Electron-beam drilled sites		Machine drilled sites	
Site radius, R_c, in.	Surface- to saturation-temperature difference, $(\Delta T)_i$, ^oF	Site radius, R_c, in.	Surface- to saturation-temperature difference, $(\Delta T)_i$, ^oF	Site radius, R_c, in.	Surface- to saturation-temperature difference, $(\Delta T)_i$, ^oF	Site radius, R_c, in.	Surface- to saturation-temperature difference, $(\Delta T)_i$, ^oF
0.0024	4.4	0.0015	10.4	0.0037	3.4	0.0055	11.2
.0024	4.4	.0015	6.4	.0037	7.5	.0057	5.8
.0025	11.3	.0015	7.1	.0037	4.6	.0057	11.2
.0025	12.1	.0016	10.3	.0043	3.8	.0057	8.1
.0032	4.5	.0016	6.4	.0043	2.9	.0057	5.7
0.0032	4.5	0.0016	7.1	0.0044	3.1	0.0061	12.0
.0034	6.0	.0019	5.8	.0044	3.3	.0061	9.4
.0034	7.5	.0019	6.7	.0045	8.4	.0063	10.4
.0034	6.7	.0027	9.4	.0047	7.4	.0072	8.1
.0034	11.2	.0027	8.7	.0047	7.9	.0072	9.0
0.0036	7.4	0.0034	7.0	0.0047	8.0	0.0078	10.4
.0036	7.9	.0034	9.5	.0047	7.5	.0078	9.0
.0036	8.0	.0034	8.7	.0047	3.4	.0078	8.1
.0036	7.5	.0036	9.5	.0047	10.9	.0103	11.5
.0037	3.0	.0036	7.6			.0105	7.8
		0.0037	9.5			0.0105	12.1
		.0037	7.6			.0106	10.2
		.0038	12.0			.0106	13.0
		.0038	7.1			.0107	11.5
		.0038	6.2			.0152	13.0
		0.0044	7.0			0.0152	14.4
		.0046	7.9			.0207	7.8
		.0046	10.0			.0215	14.4
		.0050	10.0			.0215	13.0
		.0050	7.9			.022	10.7
		.0055	7.9			.032	14.0
		.0055	5.8			.032	10.4

TABLE II. - BUBBLE DIMENSIONS AND FORCES AT ONSET OF BUBBLE DEPARTURE IN SATURATED WATER

[Mechanically drilled sites.]

Bubble diameter, D, in.	Bubble height, H, in.	Diameter of drilled site, D_c, in.	Depth of drilled site, in.	Bubble volume, V, $in.^3$	Buoyancy force, F_B, lb	Surface tension force, F_T, lb
0.1208	0.181	0.0413	0.030	1.18×10^{-3}	4.74×10^{-5}	4.34×10^{-5}
.1181	.176	↓	↓	1.11	4.55	↓
.1144	.169			1.00	4.25	
.1112	.162			.921	4.06	
.1097	.159			.885	3.98	
.1079	.156			.844	3.87	
.1040	.148	↓		.751	3.65	↓
.1066	.157	.0304		.796	3.27	3.19
.1035	.146	.0304	↓	.726	3.09	3.19
.0965	.133	.0209	.020	.560	2.26	2.19
.0951	.130	.0209		.540	2.21	2.19
.0829	.106	.0209		.358	1.67	2.19
.0791	.100	.0114		.298	1.17	1.20
.0775	.0968	.0114	↓	.298	1.17	1.20
.0701	.0873	.0076	.010	.207	.790	.798
.0599	.0720	.0076		.123	.515	.798
.0782	.0985	.0075		.278	1.021	.787
.0775	.0970	↓		.270	.997	↓
.0768	.0945			.270	.999	
.0759	.0945			.252	.939	
.0734	.0910			.227	.860	
.0708	.0870	↓		.205	.784	↓
.0514	.0586	.0038		.0763	.291	.399
.0462	.0508	.0038	↓	.0529	.214	.399

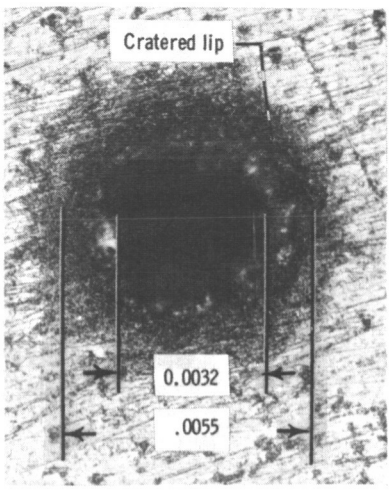

(a) Obtained by electron-beam disintegration; depth, 0.0025 inch. 250X.

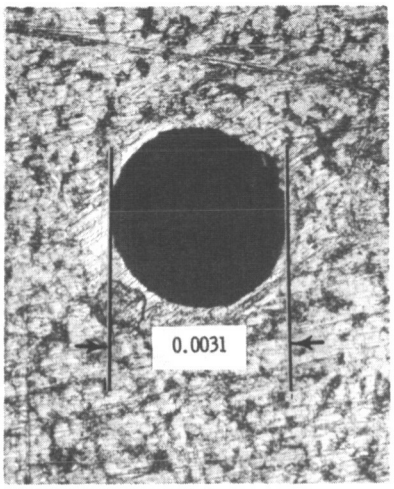

(b) Obtained by mechanical drill; depth, 0.010 inch. 290X.

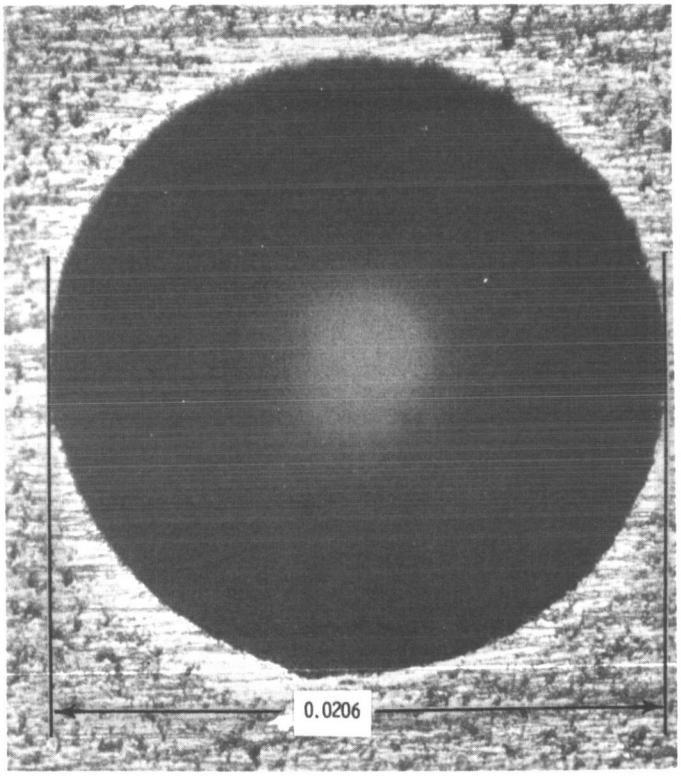

C-66-691

(c) Obtained by mechanical drill; depth, 0.020 inch. 150X.

Figure 1. - Artificial nucleation sites. (All dimensions in inches.)

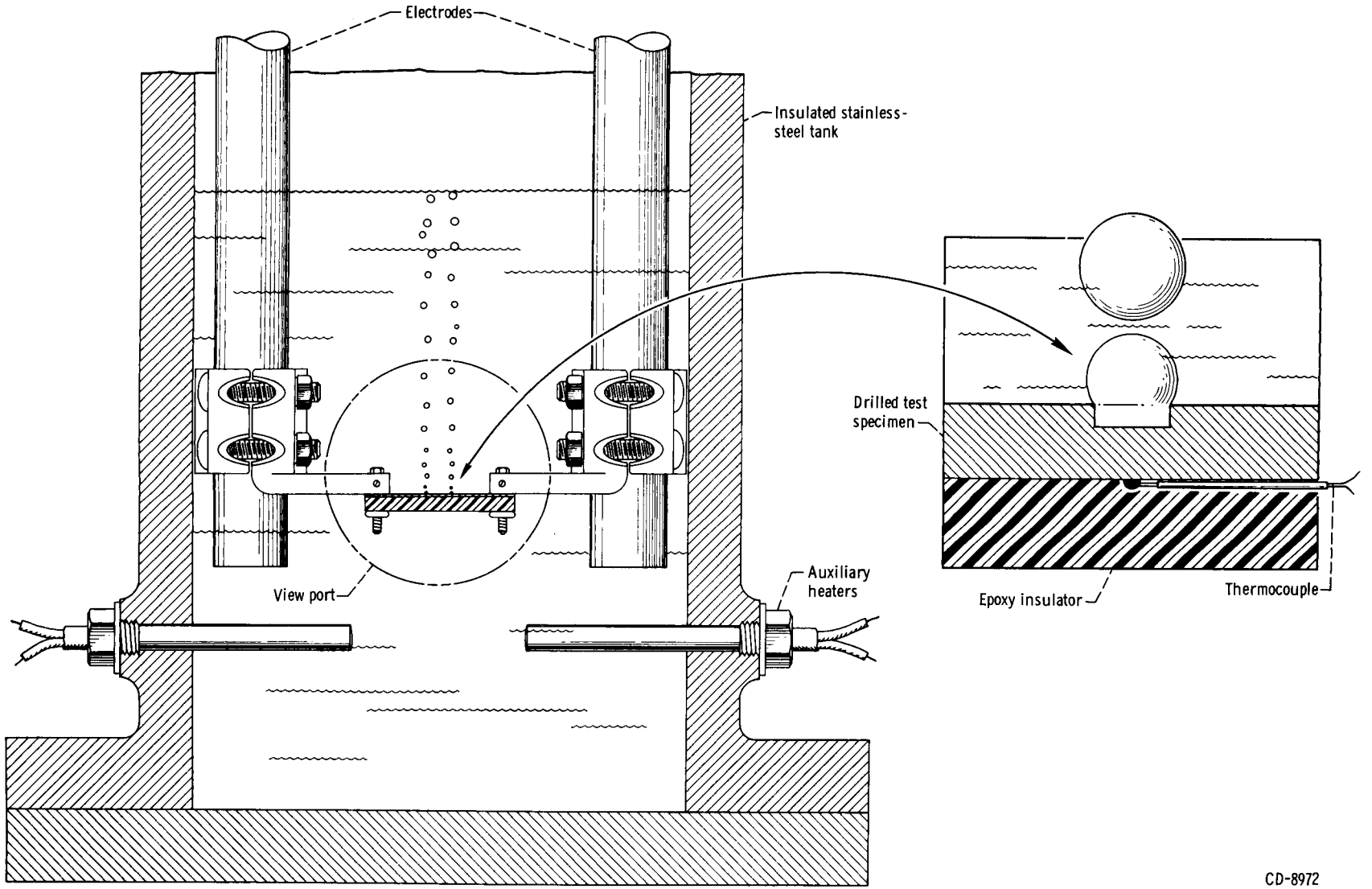

Figure 2. - Schematic diagram of experimental apparatus.

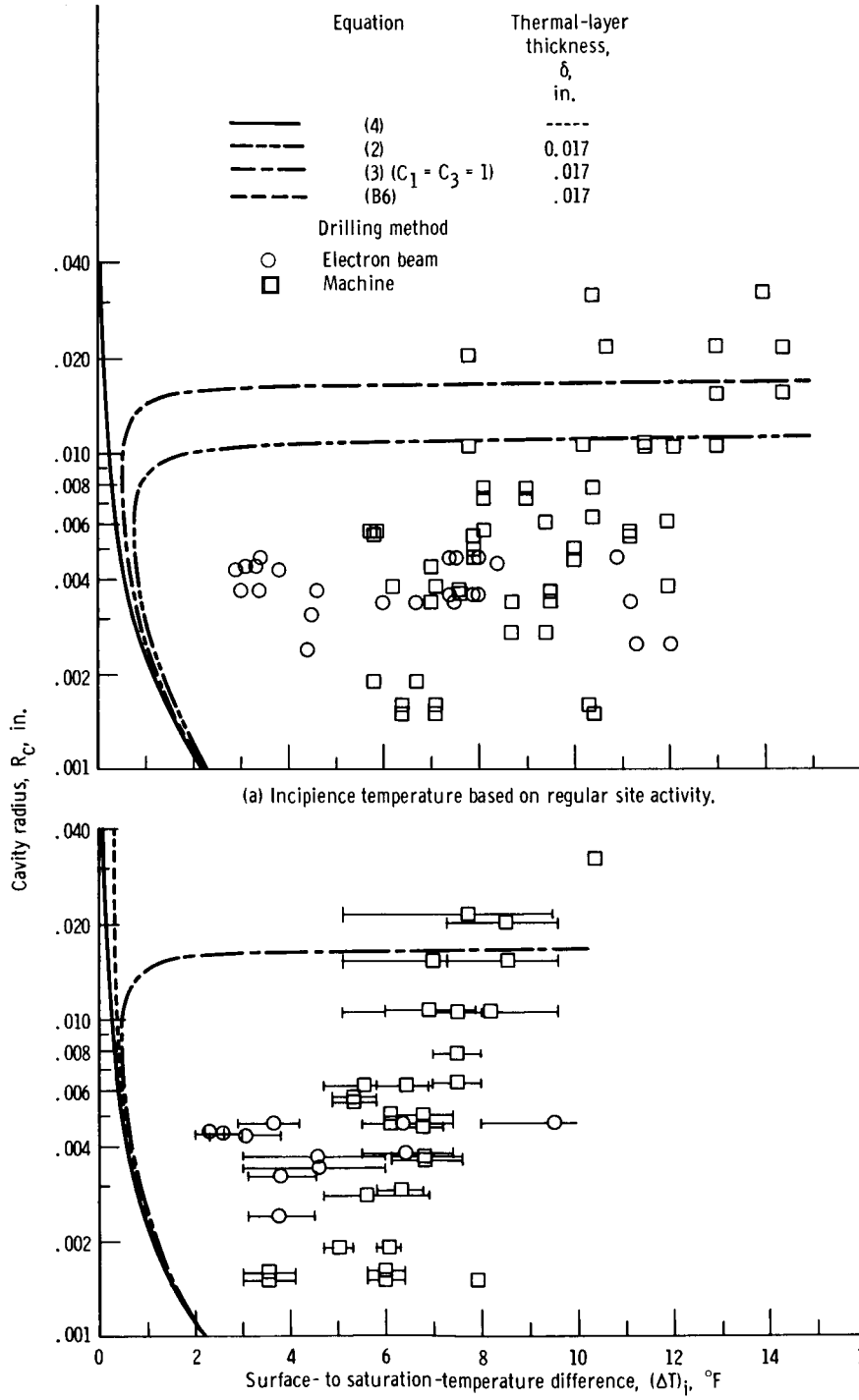

(a) Incipience temperature based on regular site activity.

(b) Incipience temperature range from where there are few bursts of bubbles to where bubble detachment ceases.

Figure 3. - Temperature difference required to initiate bubbles from artificial sites in water at saturation temperature.

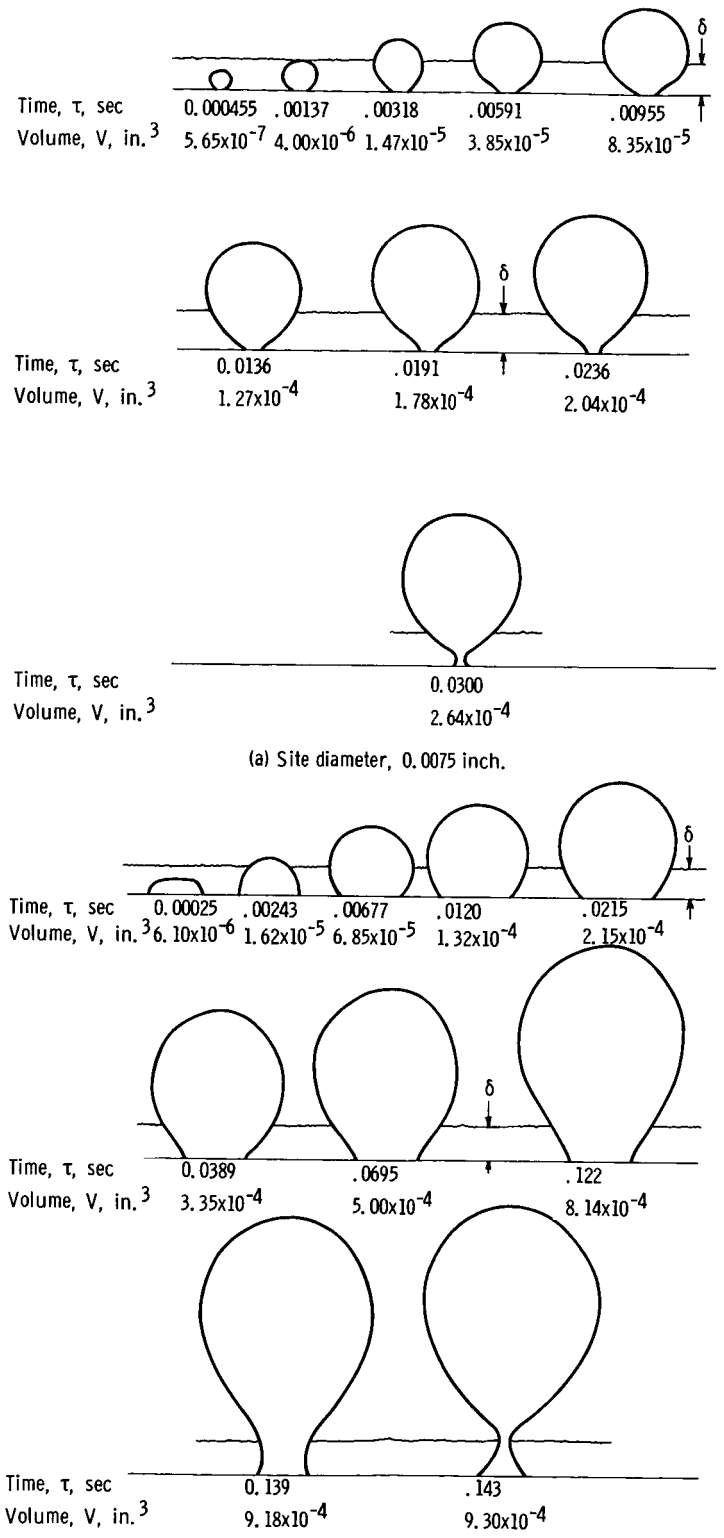

(a) Site diameter, 0.0075 inch.

(b) Site diameter, 0.0413 inch.

Figure 4. - Growth profiles of bubbles at artificial site. Temperature difference ΔT, 12.5° F; thermal layer thickness δ, 0.017 inch; heat flux q, 7100 Btu per hour per square foot.

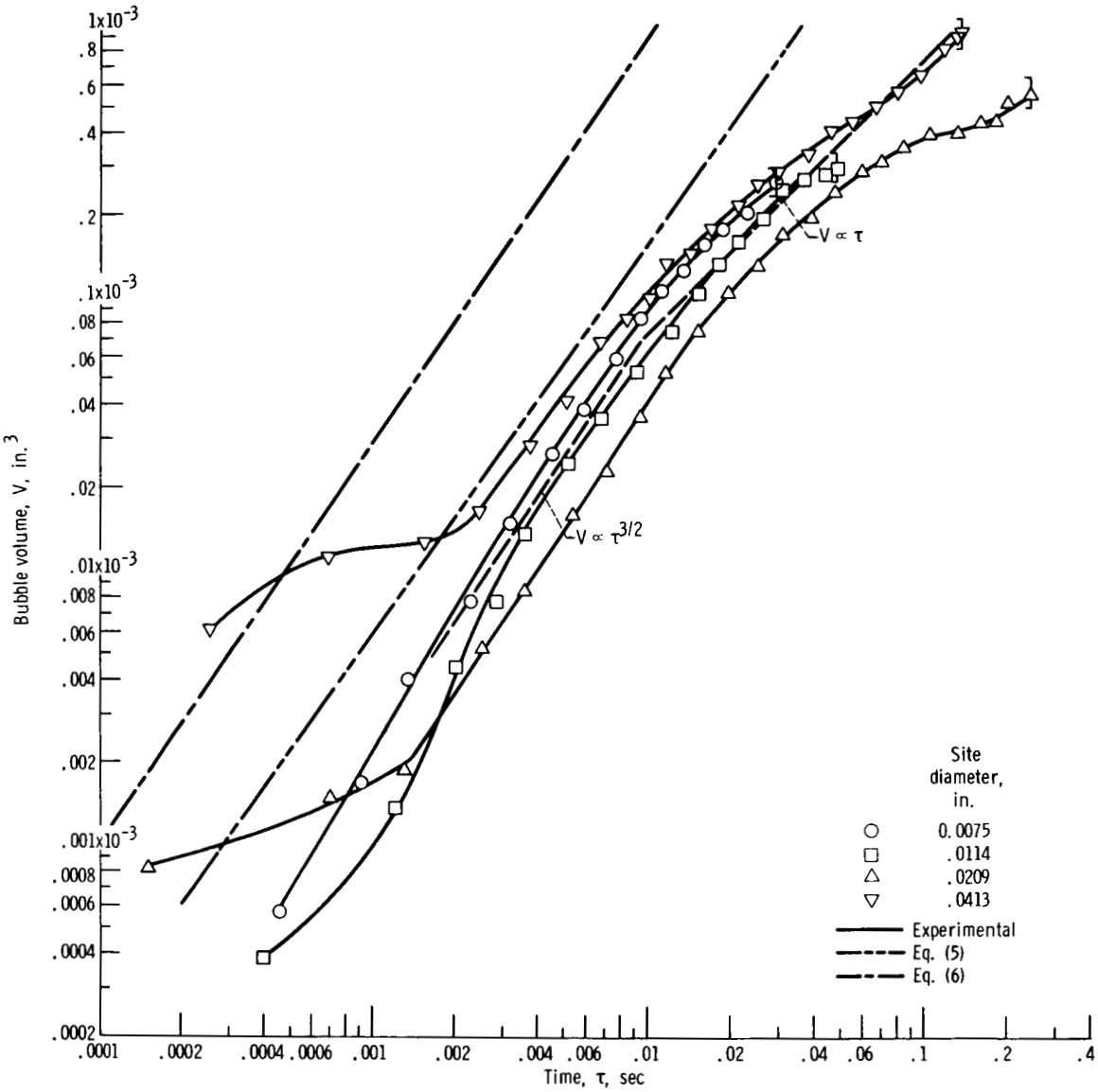

Figure 5. - Effect of nucleation site size on bubble-growth rates. Temperature difference ΔT, 12.5° F; heat flux from surface q, 7100 Btu per hour per square foot.

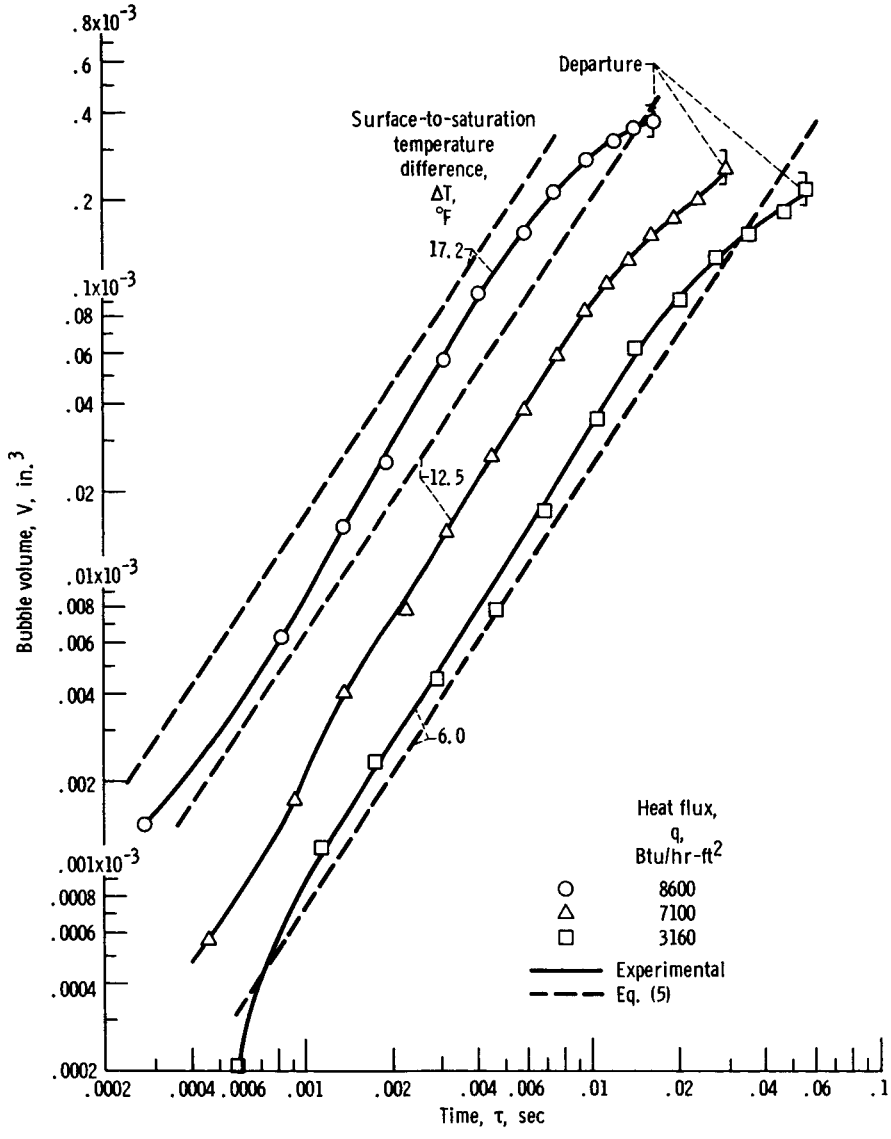

(a) Site diameter, 0.0075 inch.

Figure 6. - Effect of surface- to saturation-temperature difference on bubble-growth rates from artificial sites.

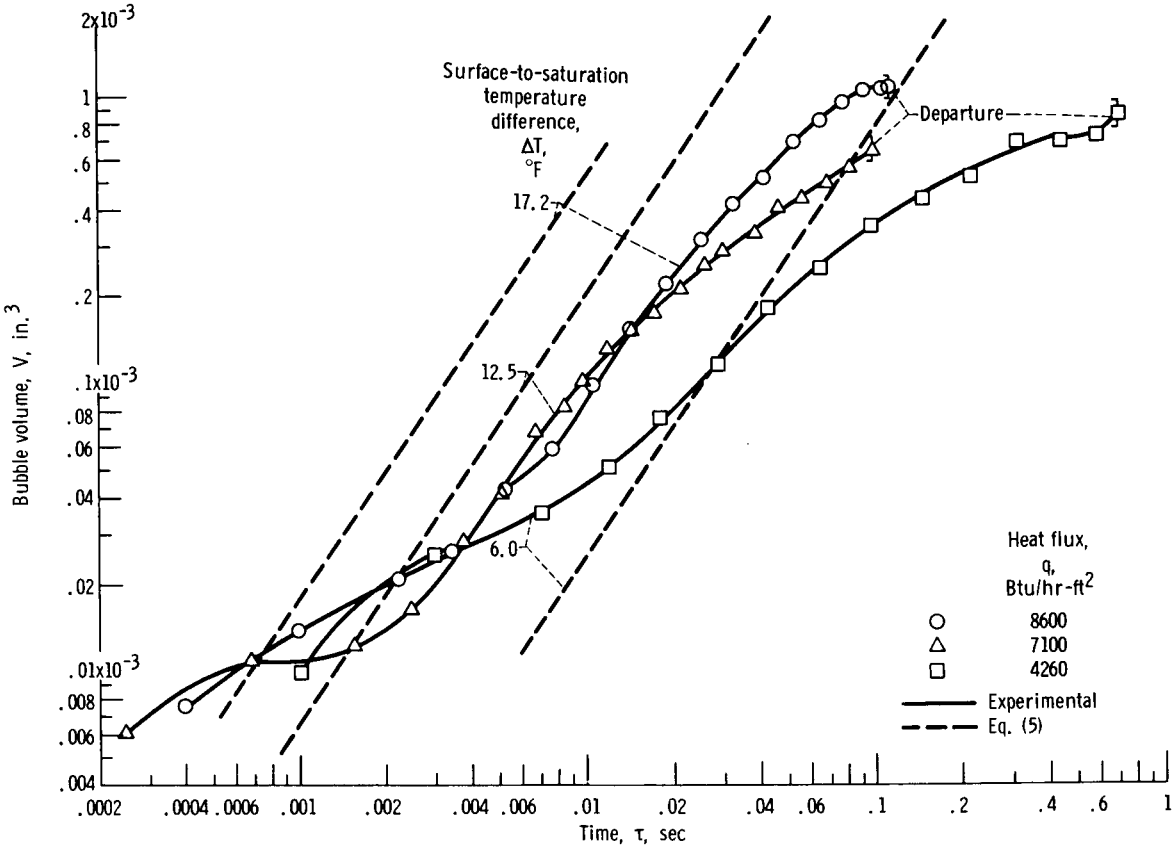

(b) Site diameter, 0.0413 inch.

Figure 6. - Concluded.

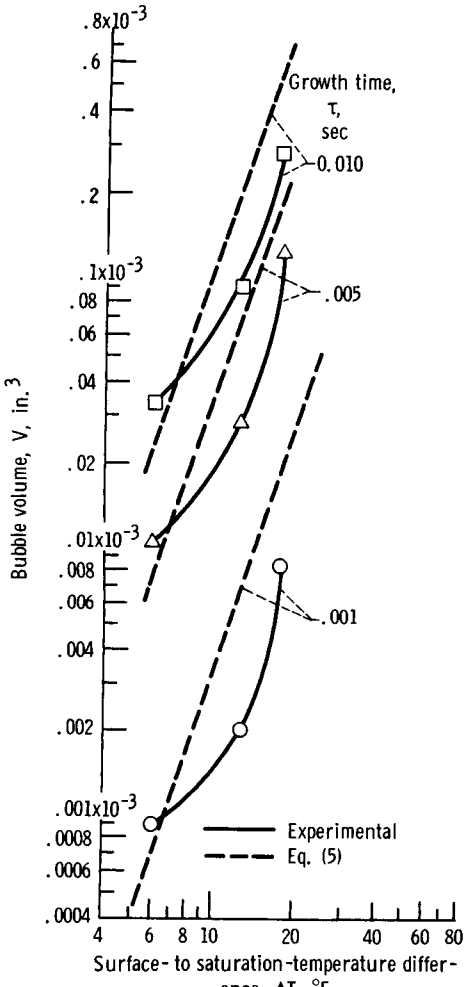

Figure 7. - Effect of surface- to saturation-temperature difference on bubble growth rates from artificial sites. Site diameter, 0.0075 inch.

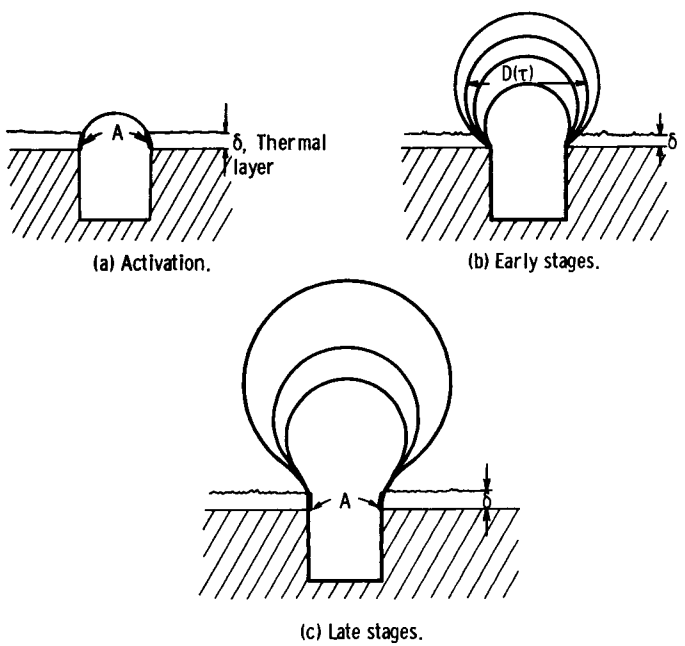

Figure 8. - Stages in growth of bubble from artificial site.

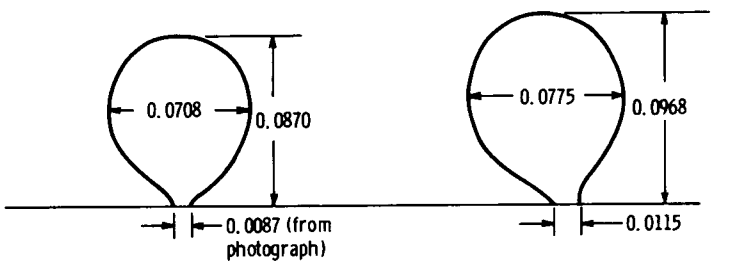

(a) Volume, 2.05×10^{-4} inch^3; site diameter, 0.0075 inch (from microscope).

(b) Volume, 2.98×10^{-4} inch^3; site diameter, 0.0114 inch (from microscope).

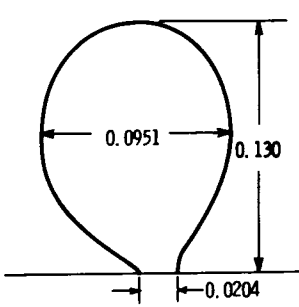

(c) Volume, 5.40×10^{-4} inch^3; site diameter, 0.0209 inch (from microscope).

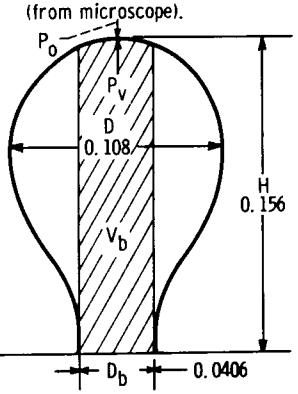

(d) Volume, 8.44×10^{-4} inch^3; site diameter, 0.0413 inch (from microscope).

Figure 9. - Typical bubble configurations just prior to necking and departure. Temperature difference, ΔT, 12.5° F. (All dimensions in inches.)

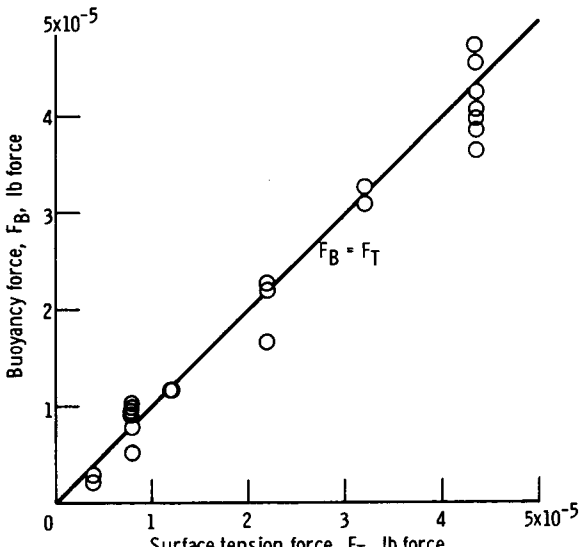

Figure 10. - Comparison of buoyancy and surface-tension forces acting on bubbles at onset of departure.

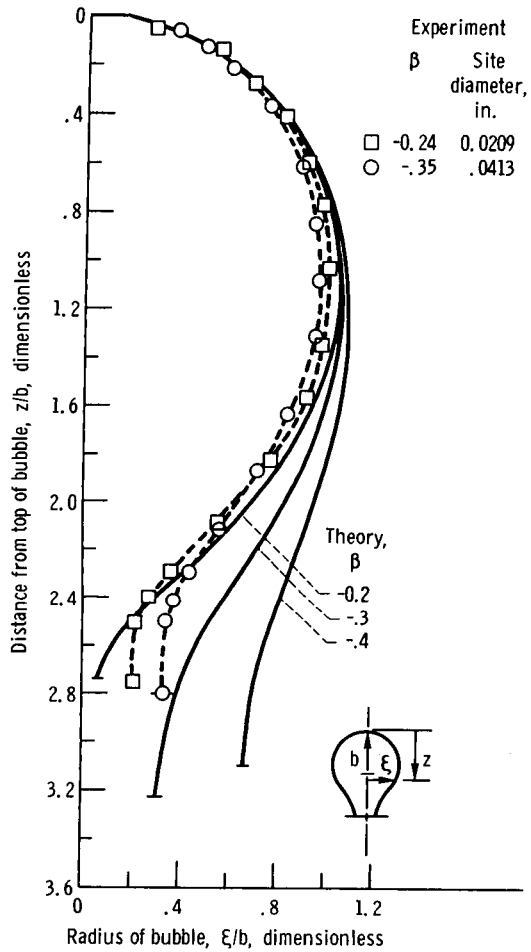

Figure 11. - Comparison of theoretical and experimental bubble profiles at onset of bubble departure when buoyancy and surface tension forces are in equilibrium. Temperature difference, ΔT, 12.5° F.

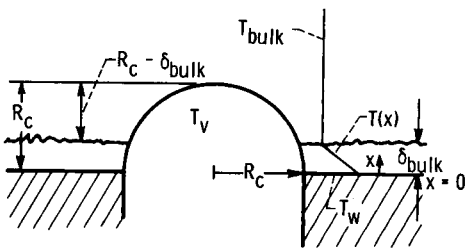

(a) Nucleus extending outside thermal layer.

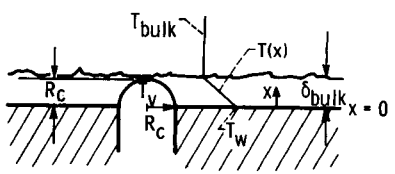

(b) Nucleus contained within thermal layer.

Figure 12. - Criteria for growth of hemispherical bubble nucleus.

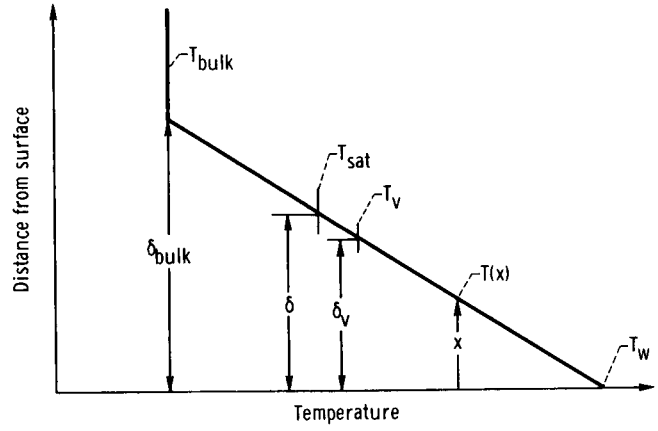

Figure 13. - Significant temperatures and thicknesses in thermal layer.

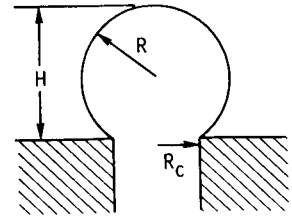

Figure 14. - Truncated sphere bubble model.

NASA-Langley, 1967 —— 33 E-3189

8/10/67

"The aeronautical and space activities of the United States shall be conducted so as to contribute . . . to the expansion of human knowledge of phenomena in the atmosphere and space. The Administration shall provide for the widest practicable and appropriate dissemination of information concerning its activities and the results thereof."

—NATIONAL AERONAUTICS AND SPACE ACT OF 1958

NASA SCIENTIFIC AND TECHNICAL PUBLICATIONS

TECHNICAL REPORTS: Scientific and technical information considered important, complete, and a lasting contribution to existing knowledge.

TECHNICAL NOTES: Information less broad in scope but nevertheless of importance as a contribution to existing knowledge.

TECHNICAL MEMORANDUMS: Information receiving limited distribution because of preliminary data, security classification, or other reasons.

CONTRACTOR REPORTS: Scientific and technical information generated under a NASA contract or grant and considered an important contribution to existing knowledge.

TECHNICAL TRANSLATIONS: Information published in a foreign language considered to merit NASA distribution in English.

SPECIAL PUBLICATIONS: Information derived from or of value to NASA activities. Publications include conference proceedings, monographs, data compilations, handbooks, sourcebooks, and special bibliographies.

TECHNOLOGY UTILIZATION PUBLICATIONS: Information on technology used by NASA that may be of particular interest in commercial and other non-aerospace applications. Publications include Tech Briefs, Technology Utilization Reports and Notes, and Technology Surveys.

Details on the availability of these publications may be obtained from:

SCIENTIFIC AND TECHNICAL INFORMATION DIVISION

NATIONAL AERONAUTICS AND SPACE ADMINISTRATION

Washington, D.C. 20546